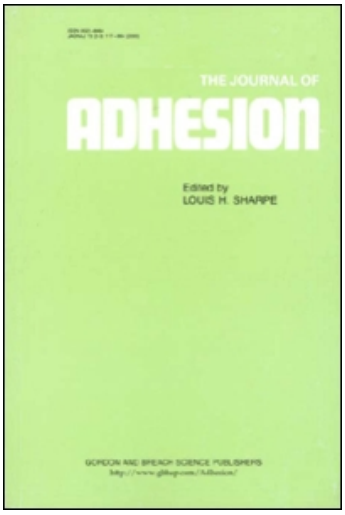

The Journal of Adhesion

Publication details, including instructions for authors and subscription information:
http://www.informaworld.com/smpp/title~content=t713453635

Elastic Fracture Mechanics of the Peel-Test Geometry

M. D. Thouless[a]; H. M. Jensen[b]
[a] IBM Research Division, T. J. Watson Research Center, Yorktown Heights, NY, USA [b] Department of Solid Mechanics, The Technical University of Denmark, Lyngby, Denmark

To cite this Article Thouless, M. D. and Jensen, H. M.(1992) 'Elastic Fracture Mechanics of the Peel-Test Geometry', The Journal of Adhesion, 38: 3, 185 — 197
To link to this Article: DOI: 10.1080/00218469208030454
URL: http://dx.doi.org/10.1080/00218469208030454

J. Adhesion, 1992, Vol. 38, pp. 185–197
Reprints available directly from the publisher
Photocopying permitted by license only

Printed in the United Kingdom

Elastic Fracture Mechanics of the Peel-Test Geometry

M. D. THOULESS

IBM Research Division, T. J. Watson Research Center, Yorktown Heights, NY 10598, USA

H. M. JENSEN

Department of Solid Mechanics, The Technical University of Denmark, DK-2800 Lyngby, Denmark

(Received January 28, 1992; in final form March 11, 1992)

The results of a linear-elastic analysis to determine the phase angle at the tip of an interface crack in the peel test are presented in this paper. The phase angle is fairly insensitive to the peel angle and, when the film and substrate have identical elastic properties, the mode-I and mode-II components of the crack-tip stress field are approximately equal. The phase angle has some dependence on both the elastic mismatch and the applied force; it is very sensitive to any residual strains in the film.

KEY WORDS peel test; fracture mechanics; mixed-mode fracture; peel angle; phase angle; residual strain; stress-intensity factor; energy-release rate.

1 INTRODUCTION

The peel test has been used for many decades as a convenient and relatively simple means of characterising adhesion. The test consists of measuring the force required to peel a film from a substrate. This force is termed the peel force and, at the simplest level, the adhesion of a film is sometimes quoted in terms of this force. Such a measure of adhesion, however, has no utility beyond providing a reference with which to compare other nominally identical films loaded in an identical fashion. A more sophisticated approach uses the peel force to calculate a value for the toughness of the film-substrate interface. Under rather limited conditions, this value can then be used to predict the strength of identical interfaces under different loading geometries.

During the years that it has been used as an industrial test, there have been a number of analyses of the peel test. Initial calculations for the peel geometry treated the film as an elastic beam attached to an elastic foundation which represented the interaction (often assumed to be an adhesive) between the film and substrate. The interface crack was assumed to advance when the maximum stress in the elastic foundation reached a value identified with the strength of the adhesive.[1–4] Other

calculations used an energy-balance approach to deduce the relationship between the toughness of the interface and the peel force.[5-7] Many of these analyses assumed that the film deformed in a linear-elastic fashion, but some incorporated visco-elastic[7-8] and elasto-plastic[9-15] effects. Indeed, one of the more severe limitations to the peel test is that large stresses and bending deformations may occur that can result in significant deviations from linear behaviour. This has been carefully considered and analysed in a series of recent papers by Kim, Aravas, and co-workers.[12-15]

In the general field of interfacial fracture, many studies have suggested that the measured toughness of an interface may depend on the degree of symmetry of the crack-tip stress field.[16-22] Since these "mixed-mode" effects have not been considered in more than a cursory fashion for the peel test, the present paper presents an analysis of the crack-tip stress fields for this geometry. The calculations assume linear elasticity and, therefore, their utility is limited to hard films subjected to relatively low peel forces. Despite this caveat, the solutions are rigorous in the sense that they allow for large axial deformations within the film (provided that these remain linear), and they are valid for any general combination of elastic properties of the film and substrate.

2 THEORY

2.1 Fundamental Solution for Thin-Film Delamination

The fundamental problem that underlies many aspects of the mechanics of thin-film delamination has been analysed by Suo and Hutchinson,[23-24] and is illustrated in Fig. 1. Any arbitrary set of loads that may act so as to cause the film to delaminate can be represented by a single force, P_o, per unit width, acting along the neutral axis of the film, and a bending moment, M_o, per unit width, provided that the crack tip is sufficiently far removed from the edge of the sample or from other points of application of the loads. If the loads are applied externally, then P_o and M_o are directly related to them. If the film is under a residual stress, then P_o and M_o represent the loads that must be applied to relax this stress.

For a plane geometry, in which the substrate is infinitely thick and both the substrate and film are isotropic elastic solids, the energy-release rate at the tip of the crack in Fig. 1 is given by[24]

$$\mathcal{G} = (P_o^2 + 12M_o^2/h^2)/2\hat{E}_1 h \tag{1}$$

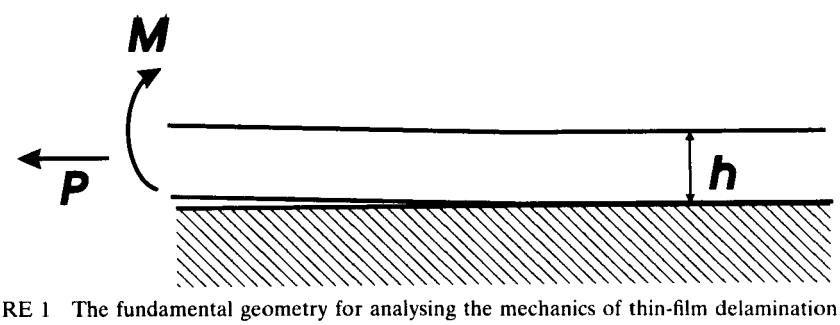

FIGURE 1 The fundamental geometry for analysing the mechanics of thin-film delamination.

where h is the film thickness, $\hat{E}_1 = E_1$, the Young's modulus of the film in plane stress, $\hat{E}_1 = E_1/(1-\nu_1^2)$ in plane strain, and ν_1 is Poisson's ratio of the film. The stress-intensity factor, K, is related to M_o and P_o by[24]

$$Kh^{i\epsilon} = -\left[\frac{3(1-\alpha)}{1-\beta^2}\right]^{1/2} [1 + i(12)^{1/2}(M_o/P_o h)] e^{i\omega} P_o h^{-1/2} \tag{2}$$

where

$$\epsilon = \frac{1}{2\pi} \ln\left(\frac{1-\beta}{1+\beta}\right),$$

ω, a function of α and β, is given by Suo and Hutchinson,[23] and α and β are the Dundurs' parameters for the mismatch between the film and substrate:

$$\alpha = \frac{\hat{E}_1 - \hat{E}_2}{\hat{E}_1 + \hat{E}_2}$$

$$\beta = \frac{\mu_1(\kappa_2 - 1) - \mu_2(\kappa_1 - 1)}{\mu_1(\kappa_2 + 1) + \mu_2(\kappa_1 + 1)},$$

where μ is the shear modulus, $\kappa = 3 - 4\nu$ in plane strain, $\kappa = (3-\nu)/(1+\nu)$ in plane stress, and the subscripts 1 and 2 refer to the film and substrate, respectively. The phase angle, ψ, which relates the real and imaginary parts of equation (2) is given by[24]

$$\tan\psi = \frac{Im(Kh^{i\epsilon})}{Re(Kh^{i\epsilon})} = \frac{(12)^{1/2}(M_o/P_o h) + \tan\omega}{-(12)^{1/2}(M_o/P_o h)\tan\omega + 1} \tag{3}$$

In the special case when $\beta = 0$, equation (2) gives the conventional mode-I and mode-II stress-intensity factors, K_I and K_{II}, respectively:

$$K_I + iK_{II} = -[3(1-\alpha)]^{1/2}[1 + i(12)^{1/2}(M_o/P_o h)] e^{i\omega} P_o h^{-1/2} \tag{4}$$

The phase angle is then

$$\psi = \tan^{-1}(K_{II}/K_I) \tag{5}$$

The results of Ref. [24], therefore, reduce the analysis of any thin-film delamination problem to one of determining P_o and M_o. This approach is used for the peel test in the following section.

2.2 Peel Test

The macroscopic geometry for the peel test is shown in Fig. 2. A force, P_∞, per unit width, is applied to the film at a large distance from the substrate and at an angle θ to it. A simple consideration of the energy changes that occur as the film delaminates allows the energy-release rate to be calculated as[6]

$$\mathcal{G} = \frac{P_\infty^2}{2\hat{E}_1 h} + P_\infty(1 - \cos\theta) \tag{6}$$

The applied force, P_∞, acts so as to produce a force P_o and a bending moment M_o

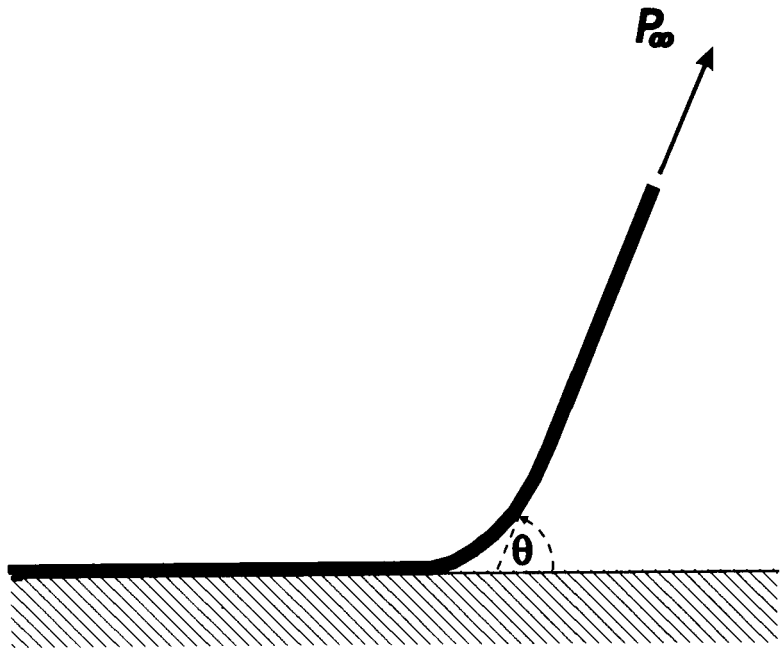

FIGURE 2 The peel-test geometry.

in the region of the crack tip as illustrated in Fig. 1. Considerations of equilibrium allow a relationship between P_o and P_∞ to be written down as

$$P_o = P_\infty \cos\theta \tag{7}$$

Equations (1), (6) and (7) can be combined to obtain an expression for M_o:

$$M_o = \left[\frac{\hat{E}_1 h^3}{6}\left(\frac{P_\infty^2 \sin^2\theta}{2\hat{E}_1 h} + P_\infty(1-\cos\theta)\right)\right]^{1/2} \tag{8}$$

So that, from equation (3),

$$\tan\psi = \frac{[\sin^2\theta + 2(1-\cos\theta)/\epsilon_\infty]^{1/2} + \tan\omega\cos\theta}{-\tan\omega[\sin^2\theta + 2(1-\cos\theta)/\epsilon_\infty]^{1/2} + \cos\theta} \tag{9}$$

where $\epsilon_\infty = P_\infty/\hat{E}_1 h$ and can be considered to be the applied strain. As $\epsilon_\infty \to 0$, this equation reduces to

$$\tan\psi = \frac{[2(1-\cos\theta)/\epsilon_\infty]^{1/2} + \tan\omega\cos\theta}{-\tan\omega[2(1-\cos\theta)/\epsilon_\infty]^{1/2} + \cos\theta} \tag{10}$$

3 DISCUSSION

3.1 Phase Angle

The results of the previous section can be used to illustrate some aspects of the peel test. For ease of presentation, attention is limited to systems for which the film and

substrate have identical elastic parameters, *i.e.*, the Dundurs' parameters, α and β, are both equal to zero, and the Young's modulus of the film and substrate are both given by E. The effect of non-zero values for the Dundurs' parameters is reflected simply by a change in ω. When $\alpha = \beta = 0$, $\omega = 52.1°$[23] and the phase angle is given by (Eqn. 9)

$$\psi = \tan^{-1}\left\{\frac{[\sin^2\theta + 2(1-\cos\theta)/\epsilon_\infty]^{1/2} + 1.286\cos\theta}{-1.286[\sin^2\theta + 2(1-\cos\theta)/\epsilon_\infty]^{1/2} + \cos\theta}\right\} \tag{11}$$

This function is plotted in Fig. 3 for a range of ϵ_∞. The sign of ψ has been chosen with the convention that the mode-II component of the stress-intensity factor acts so as to give a tendency for the crack to propagate into the film when ψ is less than zero. ψ is always negative, so, unless the film has a substantially higher fracture resistance than the interface, one should expect the film to fracture.[25-26]

A surprising result illustrated in Fig. 3 is that the phase angle is fairly insensitive to the peel angle. The degree of this insensitivity increases as the applied load decreases until, in the limit of $\epsilon_\infty = 0$, the phase angle is constant and equal to $-37.9°$ for all peel angles. In particular, it should be noted that the configuration sometimes referred to as the "$\pi/2$ peel-test" (*i.e.*, $\theta = 90°$) is certainly not the pure mode-I test it is occasionally claimed to be. Indeed, it would appear to be impossible to devise a peel test that would allow one to investigate fracture under pure mode-I conditions in the absence of any residual strains within the film (see Section 3.4).

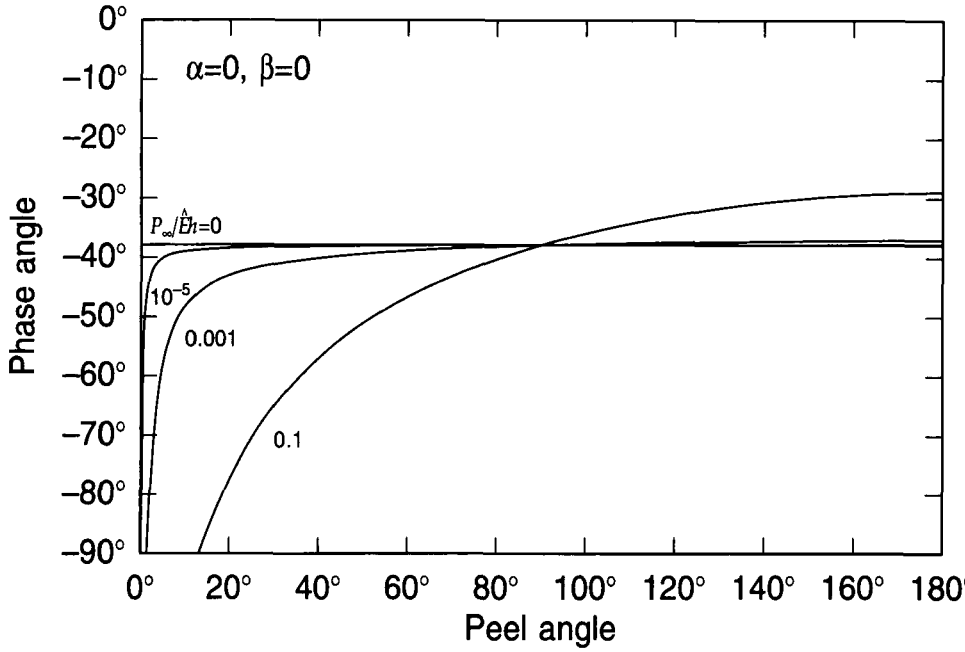

FIGURE 3 Phase angle as a function of peel angle for various peel strains. (This figure corresponds to the case when there is no elastic mismatch between the film and substrate.)

A second result, emphasised in Fig. 4, is that the phase angle equals $-90°$ at a critical peel angle which depends on ϵ_∞. This corresponds to a situation in which pure mode-II acts at the crack tip. If the peel angle is less than this critical value, the surfaces of the crack near its tip will be forced into contact. Such a phenomenon has been observed experimentally.[7] Any analysis of fracture under these conditions must include the effects of frictional interactions between the crack surfaces within the crack-tip contact zone.[27-28] If θ is larger than the critical value, K_I will be positive and the crack will be open to its tip.

3.2 Limit of Applicability of Elastic Fracture-Mechanics

The analysis presented in this paper is valid only under conditions of small-scale yielding. There are two possible sources of plasticity in a peel test which may act so as to cause errors in any interpretation of the data. The first is yielding of the

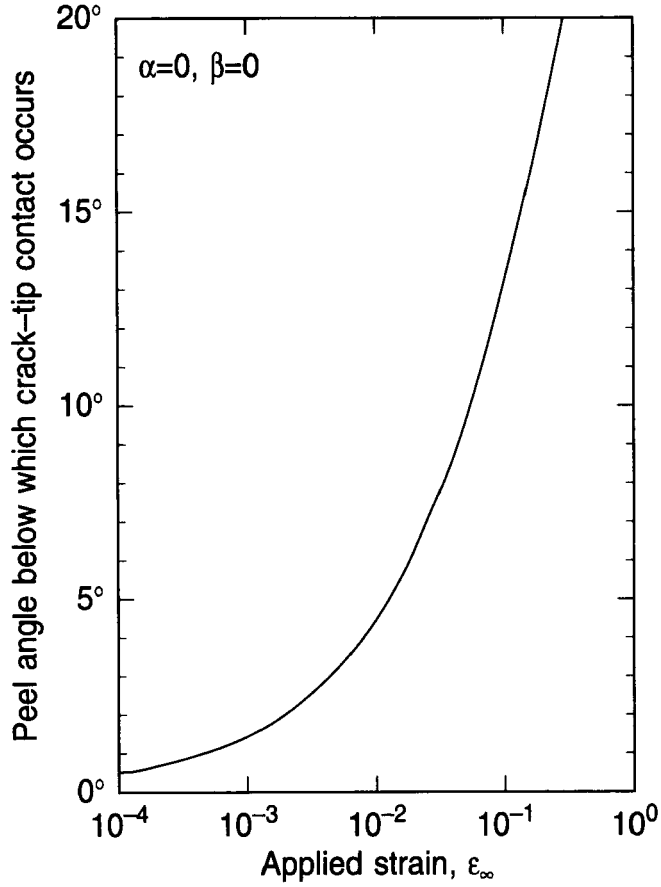

FIGURE 4 The peel angle below which crack-tip contact occurs, as a function of the peel force. (No elastic mismatch between the film and substrate.)

detached film caused by the applied force; the second is if the interface has a sufficiently high fracture resistance that the size of any non-linear region associated with the crack-tip stress field becomes significant with respect to the film thickness.

The condition to ensure that deformation of the detached film is always elastic is that the sum of the absolute values of the maximum bending stress and the axial stress associated with the applied force must not exceed the yield stress of the film, *i.e.*,

$$\frac{6M_o}{h^2}+\frac{P_\infty|\cos\theta|}{h}\leq Y\,. \tag{12}$$

This condition, upon substitution of equation (8) into it, becomes

$$[3\sin^2\theta-\cos^2\theta]\epsilon_\infty^2+[6(1-\cos\theta)+2(Y/\hat{E})|\cos\theta|]\epsilon_\infty-(Y/\hat{E})^2\leq 0 \tag{13}$$

and is used to plot Fig. 5 which shows how the maximum permissible value of P_∞ varies with θ. In the limit of $Y/E\to 0$, equation (13) gives the condition

$$\epsilon_\infty\leq(Y/\hat{E})^2/[6(1-\cos\theta)] \tag{14}$$

When $\theta=90°$, this equation further reduces to one derived by Kim *et al.*[12-14]

The validity of the "small-scale yielding" assumption can be estimated from standard empirical criteria for ensuring the validity of a fracture test.[29] For thin-film

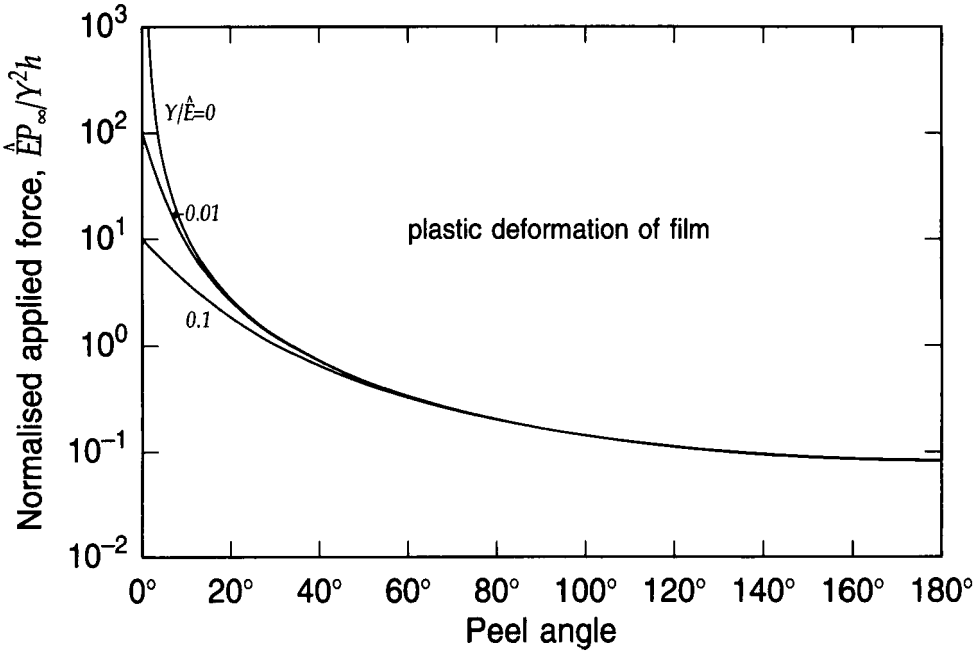

FIGURE 5 Maximum permissible value of the applied load for the stresses within the detached portion of the film to remain elastic.

geometries, the criterion that the size of the plastic zone should be small compared to the film thickness sets an approximate lower-bound on h:†

$$h \gtrsim 5\hat{E}\mathcal{G}/Y^2 \tag{15}$$

In the limit of $\epsilon_\infty \to 0$, $\mathcal{G} \simeq P_\infty(1-\cos\theta)$ and the condition for "small-scale yielding" becomes

$$\epsilon_\infty \lesssim (Y/\hat{E})^2/[5(1-\cos\theta)] \tag{16}$$

This is very similar to equation (14), so it appears that both criteria give similar limitations on the maximum value of the peel force that will allow unambiguous values of the interface toughness to be deduced. However, it is expected that minor violations of the "small-scale yielding" criterion will introduce less ambiguity into the results than will non-linear deformation of the attached film. Kim and co-workers have done extensive analyses for the mechanics involved when large-scale plasticity occurs, and have calculated the energy dissipated in the plastic deformation.[12–15]

3.3 Mixed-Mode Fracture

Experimental observations suggest that the fracture resistance of an interface generally increases with the magnitude of the phase angle.[16–22] Although the peel test is not a good geometry with which to observe the effects of phase angle on fracture (Section 3.1), for the sake of completeness this section will illustrate how the peel force might be influenced by the phase angle. As would be expected from the results of Fig. 3, the effects become more significant at low peel angles for relatively large peel forces. To examine the effect of mixed-mode fracture, an empirical relationship that relates the fracture resistance, $\Gamma(\psi)$, at a phase angle ψ to the fracture resistance under pure mode-I conditions, Γ_{Ic}, must be assumed. An example of such a relationship is

$$\Gamma(\psi) = \Gamma_{Ic}[1 + \tan^2(1-\lambda)\psi] , \tag{17}$$

which has the advantage of being able to illustrate a wide variety of behaviour by a simple change in λ. For example, $\lambda = 1$ corresponds to a criterion in which the fracture resistance is independent of ψ; the opposite extreme, when $\lambda = 0$, corresponds to a criterion in which the mode-I component must equal a critical value for fracture to occur.

The peel force, P_∞^*, is given by setting P_∞ to P_∞^* and then equating equations (6) and (17):

$$\frac{1}{2}\left(\frac{P_\infty^*}{\hat{E}h}\right)^2 + \frac{P_\infty^*}{\hat{E}h}(1-\cos\theta) - \frac{\Gamma_{Ic}}{\hat{E}h}[1+\tan^2(1-\lambda)\psi] = 0 \tag{18}$$

This can be solved for P_∞^*, and the results are plotted in Fig. 6. The peel force in

†If dislocation emission occurs in the interface ahead of the crack over a length scale that is large with respect to the film thickness, "small-scale yielding" will also be violated. This possibility is not considered here.

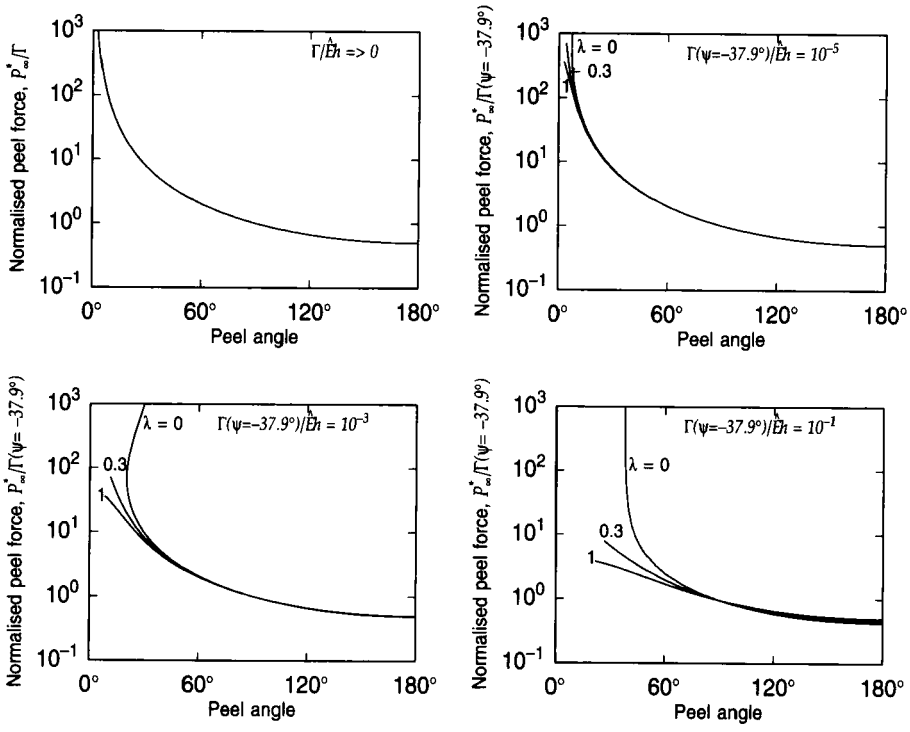

FIGURE 6 The force required to peel a film from a substrate plotted as a function of the peel angle, for different mixed-mode fracture criteria and values of interface toughness. (No elastic mismatch between the film and substrate.)

this figure has been normalised by the value of $\Gamma(\psi)$ for $\theta = 90°$ since this quantity is a more appropriate normalising parameter for the peel test than Γ_{Ic}. The limiting solution of equation (18), as $\Gamma(\psi)/\hat{E}h \to 0$, is

$$P^*_\infty/\Gamma(\psi = -37.9°) = 1/(1 - \cos\theta) \tag{19}$$

It should be emphasised that the trends predicted in this section are expected only under conditions for which the assumptions inherent in a linear-elastic, fracture-mechanics analysis are valid. If these assumptions are not met, then the variation of the peel force with the peel angle may well be dominated by large-scale non-linear effects. This appears to be the case for at least one recent study of the effect of peel force on peel angle,[30] and an analysis of the type given in Refs. 12–15 would probably be more appropriate than the present one. However, it is interesting to note that when the strain-energy term of equation (6) is not ignored, the apparent fracture resistance of the interfaces examined in Ref. 30 may be increasing as the peel angle is decreased at the smallest angles studied.

3.4 Effect of Residual Strain

The presence of a residual strain within the film influences the mechanics of the peel test in a fairly significant fashion. If the residual strain is uniform and equal to ϵ_o

throughout the film, an energy-balance calculation allows the energy-release rate to be calculated as

$$\mathcal{G} = \frac{P_\infty^2}{2\hat{E}h} + P_\infty(1-\cos\theta) - P_\infty\epsilon_o\cos\theta + \frac{\hat{E}h\epsilon_o^2}{2} \tag{20}$$

In the limit of $P_\infty/\hat{E}h \to 0$, this reduces to

$$\mathcal{G}/P_\infty = (1-\cos\theta) - \epsilon_o\cos\theta + \epsilon_o^2/2\epsilon_\infty \tag{21}$$

which, when $\theta = 90°$, is identical to the result derived by Kendall.[31] It is obvious that under this condition the effect of any residual strain is to raise the energy-release rate available to propagate an interface crack. In the absence of any dependence of the interface toughness on the phase angle, both compressive and tensile residual strains act to lower the peel force. However, the effect of a compressive residual strain on the phase angle is different from that of a tensile residual strain, and this difference may be reflected in the peel force. The phase angle can be calculated by recognising that the effective load, P_o, acting on the crack tip (Fig. 1) is given by

$$P_o = P_\infty\cos\theta - \epsilon_o\hat{E}h \tag{22}$$

so that,

$$\frac{(12)^{1/2}M_o}{P_o h} = \frac{[\sin^2\theta + 2(1-\cos\theta)/\epsilon_\infty]^{1/2}}{(\cos\theta - \epsilon_o/\epsilon_\infty)} \tag{23}$$

which can be substituted into equation (3) to obtain ψ. As an example, consider the limit of $\epsilon_\infty \to 0$, for $\alpha = \beta = 0$. Under these conditions,

$$\psi = \tan^{-1}\left[\frac{(1-\cos\theta)^{1/2} - 1.286\epsilon_o/(2\epsilon_\infty)^{1/2}}{-1.286(1-\cos\theta)^{1/2} - \epsilon_o/(2\epsilon_\infty)^{1/2}}\right], \tag{24}$$

and is plotted in Fig. 7. It should be noted that if the residual strain is compressive and has a magnitude greater than about $2.6(\epsilon_\infty)^{1/2}$ in this limit, contact will always occur at the crack tip over the entire range of possible peel angles. Over a limited range of tensile residual strains, the geometry of the peel test can be chosen so as to conduct a mode-I test. Furthermore, the change in sign of the phase angle for larger, tensile residual strains may cause a change in the crack path to one in which the crack propagates in a stable trajectory within the substrate and parallel to the interface.[32-33]

CONCLUSIONS

The insensitivity of the phase angle to the peel angle is, perhaps, the most important finding of the analysis presented in this paper. When stiff films are peeled from a substrate, the phase angle is essentially constant, except at very small peeling angles. An interfacial toughness deduced from the peel test is, therefore, expected to be fairly independent of the peel angle (assuming that conditions of small-scale plasticity are met). Only when the film is very compliant, with peel strains of almost 10%, is there any substantial effect on the phase angle. Although some experiments

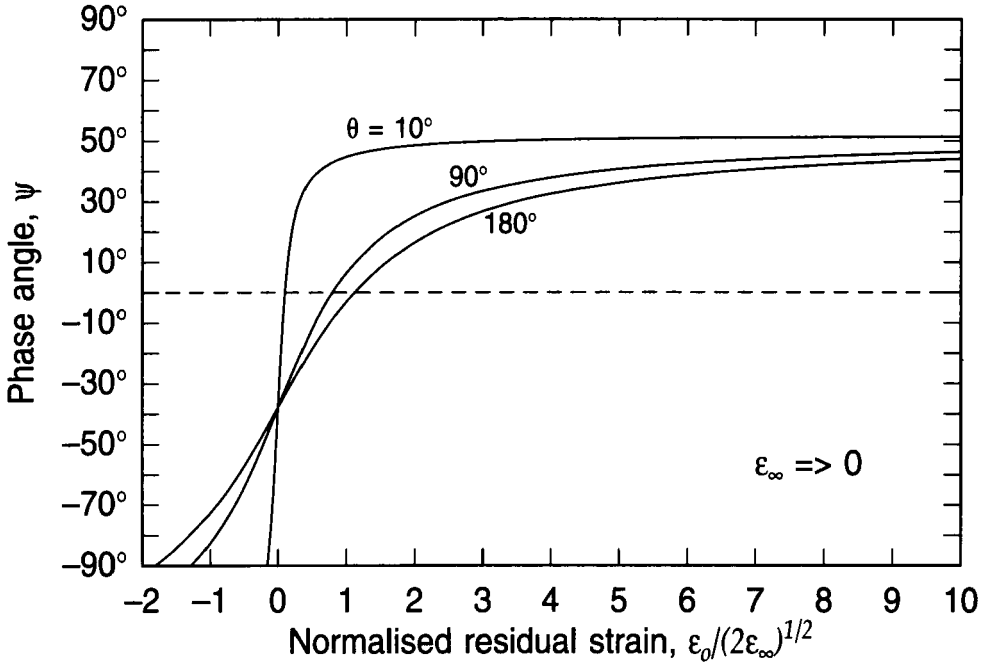

FIGURE 7 Phase angle as a function of residual strain in the film for peel angles of 10°, 90° and 180°, no elastic mismatch and in the limit of the peel strain tending to zero.

that meet this condition have been reported,[6-7] it is not possible at present to correlate these results with the theory because the combination of materials used was such that the elastic mismatch was significantly larger than the maximum mismatch for which the parameter ω in equation (9) has been calculated. Effects of the phase angle do become important at small peel angles when the analysis predicts crack-tip contact; frictional effects are then expected to have a significant influence on the apparent toughness. Furthermore, both the phase angle and the force necessary to peel a film are very sensitive to any residual strain that may exist in the film. The effects of residual strain must, therefore, be taken into consideration when interpreting the results of a peel test.

References

1. G. J. Spies, *J. Aircraft Engin.*, **25,** 64–70 (1953).
2. J. J. Bikerman, *J. Appl. Phys.*, **28,** 1484–1485 (1957).
3. A. N. Gent and G. R. Hamed, *J. Adhesion,* **7,** 91–95, (1975).
4. D. W. Nicholson, *Int. J. Fract.*, **13,** 279–287 (1977).
5. K. Kendall, *J. Phys. D,* **4,** 1186–1195 (1971).
6. K. Kendall, *J. Phys. D,* **8,** 1449–1452 (1975).
7. K. Kendall, *J. Phys. D,* **11,** 1519–1527 (1978).
8. K. Kendall, *J. Adhesion,* **5,** 105–117 (1973).
9. M. D. Chang, K. L. DeVries and M. L. Williams, *J. Adhesion,* **4,** 221 (1972).
10. W. T. Chen and T. F. Flavin, *I.B.M. J. Res. Dev.*, **16,** 203–213 (1972).
11. A. N. Gent and G. R. Hamed, *Appl. Polym. Sci.*, **21,** 2817–2831 (1977).
12. K. S. Kim and N. Aravas, *Int. J. Solids Struct.*, **24,** 417–435 (1988).

13. K. S. Kim and J. Kim, *J. Eng. Mater. Technol.*, **110,** 266–273 (1988).
14. N. Aravas, K. S. Kim and M. J. Loukis, *Mater. Sci. Eng.*, **A107,** 159–168 (1989).
15. J. Kim, K. S. Kim and Y. H. Kim, *J. Adhes. Sci. Technol.*, **3,** 175–187 (1989).
16. G. G. Trantina, *J. Comp. Mater.*, **6,** 371–385 (1972).
17. G. P. Anderson, K. L. DeVries and M. L. Williams, *J. Colloid Interf. Sci.*, **47,** 600–609 (1974).
18. R. A. Jurf and R. B. Pipes, *J. Comp. Mater.*, **16,** 386–394 (1982).
19. H. C. Cao and A. G. Evans, *Mech. Mater.*, **7,** 295–304 (1989).
20. M. D. Thouless, *Acta Metall. Mater.*, **38,** 1135–1140 (1990).
21. J. S. Wang and Z. Suo, *Acta Metall. Mater.*, **38,** 1279–1290 (1990).
22. K. M. Liechti and Y. S. Chai, *J. Appl. Mech.*, (in press).
23. Z. Suo and J. W. Hutchinson, *Int. J. Fract.*, **43,** 1–18 (1990).
24. J. W. Hutchinson and Z. Suo in *Advances in Applied Mechanics,* Vol. 29, J. W. Hutchinson and T. Y. Wu, Eds. (Academic Press, San Diego, CA, 1992), p. 64.
25. M. D. Thouless, H. C. Cao and P. A. Mataga, *J. Mater. Sci.*, **24,** 1406–1412 (1989).
26. M. Y. He and J. W. Hutchinson, *Int. J. Solids Struct.*, **25,** 1053–1067 (1989).
27. R. G. Stringfellow and L. B. Freund, *Int. J. Solids Struct,* (in press).
28. M. D. Thouless, J. W. Hutchinson and E. G. Liniger, *Acta. Metall. Mater.*, (in press).
29. M. F. Kanninen and C. H. Popelar, *Advanced Fracture Mechanics* (Oxford University Press, New York, NY, 1985).
30. A. N. Gent and S. Y. Kaang, *J. Adhesion,* **24,** 173–181 (1987).
31. K. Kendall, *J. Phys. D,* **6,** 1782–1787 (1973).
32. M. D. Thouless, A. G. Evans, M. F. Ashby and J. W. Hutchinson, *Acta Metall.*, **35,** 1333–1341 (1987).
33. Z. Suo and J. W. Hutchinson, *Int. J. Solids Struct.*, **25,** 1337–1353 (1989).
34. R. Frisch-Fry, *Flexible Bars* (Butterworths, Washington, DC, 1962).

Appendix

An alternative derivation of the phase angle can be obtained by calculating the crack-tip loads from the solutions for an elastica.[34] The normal force, shear force and bending moment, $P(s)$, $T(s)$ and $M(s)$ respectively, are functions of the arc length, s, in the peel-test geometry shown in Fig. A1. Equilibrium of an infinitesimal element requires that

$$\frac{dT(s)}{ds} + P(s)\frac{d\phi}{ds} = 0 \tag{A.1}$$

$$\frac{dP(s)}{ds} - T(s)\frac{d\phi}{ds} = 0 \tag{A.2}$$

$$\frac{dM(s)}{ds} + T(s) = 0 \tag{A.3}$$

where ϕ is the angle shown in Fig. A1. The constitutive relations, assuming linear elasticity, are

$$M(s) = \frac{\hat{E}_1 h^3}{12}\frac{d\phi}{ds} \tag{A.4}$$

$$P(s) = \hat{E}_1 h \epsilon(s) \tag{A.5}$$

where $\epsilon(s)$ is the strain in the element. From equations (A.3) and (A.4), an expression for $T(s)$ can be found which, when inserted into equation (A.2), gives

$$\frac{dP(s)}{ds} + \frac{\hat{E}_1 h^3}{12}\frac{d\phi}{ds}\frac{d^2\phi}{ds^2} = 0 \tag{A.6}$$

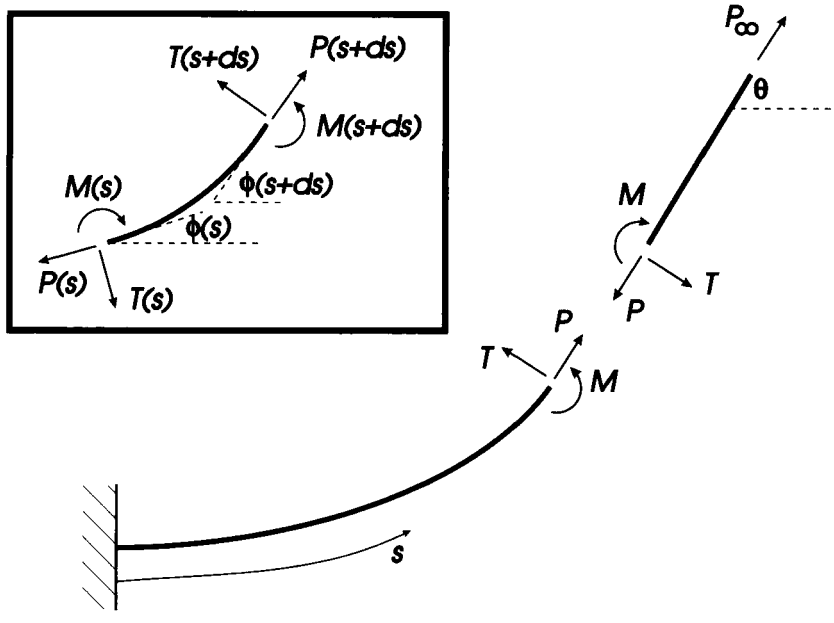

FIGURE A1 Geometry and sign conventions for the elastica solution. The inset figure shows the forces on an infinitesimal element.

After integration and substitution of equation (A.4), an expression for $P(s)$ is obtained:

$$P(s) + \frac{6M^2(s)}{\hat{E}_1 h^3} = \text{constant} \tag{A.7}$$

If the length of the film, L, is assumed to be large, the boundary conditions are $P(L) = P_\infty$ and $M(L) = 0$, giving the constant in equation (A.7). Now, at $s = 0$, overall equilibrium of the elastica gives $P_o = P_\infty \cos\theta$, and, hence, from equation (A.7),

$$M_o = (P_\infty(1 - \cos\theta)\hat{E}_1 h^3/6)^{1/2} \tag{A.8}$$

which is identical to equation (8) in the limit of $\epsilon_\infty = 0$. Using this value for M_o in equation (3) and setting $P_o = P_\infty \cos\theta$, equation (10) for the phase angle at small values of ϵ_∞ is obtained.

One other comment of interest concerns the second-order effect of the shear force which, at $s = 0$, is given by $T_o = P_\infty \sin\theta$. This effect has been ignored in the derivation of the phase angle given above, but its influence on the energy-release rate can be seen immediately by reformulating equation (6) in terms of P_o, M_o and T_o:

$$\mathcal{G} = [(P_o^2 + T_o^2) + 12M_o^2/h^2]/2\hat{E}_1 h \tag{A.9}$$

This is very similar to equation (1) with the shear force appearing as a correction term; this term can often be neglected in many applications, but not necessarily in the peel geometry.